The Company of Biologists

RESEARCH ARTICLE

The small GTPase Rab32 resides on lysosomes to regulate mTORC1 signaling

Kristina Drizyte-Miller[1], Jing Chen[2], Hong Cao[2], Micah B. Schott[2,*] and Mark A. McNiven[1,2,3,*]

ABSTRACT

Epithelial cells, such as liver-resident hepatocytes, rely heavily on the Rab family of small GTPases to perform membrane trafficking events that dictate cell physiology and metabolism. Not surprisingly, disruption of several Rab proteins can manifest in metabolic diseases or cancer. Rab32 is expressed in many secretory epithelial cells but its role in cellular metabolism is virtually unknown. In this study, we find that Rab32 associates with lysosomes and regulates proliferation and cell size of Hep3B hepatoma and HeLa cells. Specifically, we identify that Rab32 supports the mechanistic target of rapamycin complex 1 (mTORC1) signaling under basal and amino acid-stimulated conditions. Consistent with inhibited mTORC1, an increase in nuclear TFEB localization and lysosome biogenesis is also observed in Rab32-depleted cells. Finally, we find that Rab32 interacts with mTOR kinase, and that loss of Rab32 reduces the association of mTOR and mTORC1 pathway proteins with lysosomes, suggesting that Rab32 regulates lysosomal mTOR trafficking. In summary, these findings suggest that Rab32 functions as a novel regulator of cellular metabolism through supporting mTORC1 signaling.

This article has an associated First Person interview with the first author of the paper.

KEY WORDS: Small Rab GTPase, Lysosome, mTORC1, S6K, TFEB

INTRODUCTION

The small Rab GTPases comprise a family of over 60 proteins in humans that are recognized as key members of the vesicular trafficking machinery. Specific Rab proteins associate with respective intracellular compartments where they function as 'molecular switches' by cycling between GTP-bound (ON) or GDP-bound (OFF) states to support cellular endocytosis, exocytosis, intracellular vesicle and protein trafficking, and cytoskeletal dynamics (Stenmark, 2009; Zhen and Stenmark, 2015). This is particularly important for metabolism in epithelial cells, such as the liver hepatocytes that utilize this machinery to regulate lipid catabolism, nutrient uptake and secretion as well as detoxification of the blood (Schulze et al., 2019). Thus, it is not surprising that disruption of normal function of several Rab proteins is implicated in a range of metabolic diseases and cancer (Li, 2011; Li et al., 2016b; Schroeder et al., 2015; Schulze et al., 2017a,b).

In addition to Rab proteins, hepatocytes and other epithelial cells utilize an ancient signaling cascade that is highly conserved in all eukaryotes, and is considered to be a master regulator of cellular metabolism (Saxton and Sabatini, 2017). This mechanistic target of rapamycin complex 1 (mTORC1) pathway is uniquely positioned to receive inputs from nutrients, growth factors and stress, and responds accordingly to support cell growth and metabolism, whereas a related – but functionally distinct – mTORC2 integrates growth factor signaling to support cytoskeletal dynamics and cell survival (Kim and Guan, 2019). Highly metabolic organs, such as the liver, require mTORC1 signaling to support growth and regeneration (Fausto et al., 2006; Fouraschen et al., 2013; Sengupta et al., 2010), while a deregulated mTORC1 pathway has been implicated in a variety of human pathologies, such as cancers, diabetes, obesity and neurodegeneration (Laplante and Sabatini, 2012; Matter et al., 2014).

Interestingly, several Rab proteins have been found to regulate the mTORC1 signaling pathway. A genetic screen performed in *Drosophila* S2 cells revealed that knockdown of Rab5, Rab11 and Rab1 decreases phosphorylation of the well-defined mTORC1 substrate p70 ribosomal protein S6 kinase (RPS6KB1, hereafter referred to as S6K) (Li et al., 2010). Additionally, overexpression of constitutively active GTP-bound forms of Rab5 and Rab7 inactivates mTORC1 signaling, perhaps indirectly due to a disruption of endocytic trafficking (Flinn et al., 2010; Li et al., 2010). Rab1A, which supports the vesicular trafficking pathway from the endoplasmic reticulum (ER) to Golgi, is frequently overexpressed in colorectal cancer and has also been shown to activate the mTORC1 pathway (Thomas et al., 2014). Specifically, amino acids stimulate Rab1A activity and its binding with mTORC1, which then promotes mTORC1 interaction with its activator Rheb present on the Golgi apparatus, ultimately leading to increased mTORC1 activity. The contribution of other Rab GTPases to mTORC1 activity across different cells and tissue types remains poorly understood.

Rab32 was originally found to localize to mitochondria in the fibroblast-like WI-58 and COS-7 cells and, subsequently, became known for promoting the biogenesis of lysosome-related organelles, particularly pigment granule and/or melanosome biogenesis in melanocytes (Alto et al., 2002; Bultema et al., 2014; Wasmeier et al., 2006). In addition, Rab32 can associate with multiple metabolic organelles in epithelial cells, such as the ER and mitochondria-associated membranes (MAMs), where it is proposed to function as a cAMP-dependent protein kinase A-anchoring protein (AKAP), and to regulate mitochondrial dynamics and apoptosis (Bui et al., 2010). A different study suggested that its localization at the ER also supports autophagic membrane formation and autophagy under basal, nutrient-rich conditions (Hirota and Tanaka, 2009). Interestingly, the role of Rab32 in autophagy appears to be conserved in the *Drosophila* fat body, where it localizes to lysosomes and autophagosomes, and regulates lipid storage (Wang et al., 2012). Similarly, in hepatocytes,

[1]Biochemistry and Molecular Biology Program, Mayo Clinic Graduate School of Biomedical Sciences, Mayo Clinic, 200 1st Street SW, Rochester, MN 55905, USA. [2]Center for Basic Research in Digestive Diseases, Division of Gastroenterology and Hepatology, Mayo Clinic, 200 1st Street SW, Rochester, MN 55905, USA. [3]Department of Biochemistry and Molecular Biology, Mayo Clinic, 200 1st Street SW, Rochester, MN 55905, USA.

*Authors for correspondence (schott.micah@mayo.edu; mcniven.mark@mayo.edu)

K.D., 0000-0001-7049-2934; M.B.S., 0000-0002-2396-5038; M.A.M., 0000-0002-9830-1885

depletion of Rab32 results in decreased lipid droplet content, suggesting that Rab32 also regulates hepatic lipid metabolism (Li et al., 2016a). Overall, this diverse subcellular localization of Rab32 suggests that it provides a physiological link between metabolic organelles; however, its function in cellular growth and energy metabolism remains poorly understood.

In this study, we identified that the localization of Rab32 to lysosomes is particularly prevalent in primary rat hepatocytes and Hep3B human hepatoma cells. By using an unbiased reverse phase protein array screen, we found the metabolic mTORC1 signaling pathway to be markedly altered in the absence of Rab32. Subsequently, western blot analysis showed that knockdown of Rab32 inhibits both basal and amino acid-induced activation of mTORC1 signaling to S6K and, to a lesser extent, unc-51-like autophagy activating kinase 1 (ULK1). Consistent with attenuation of mTORC1 activity, we observed that Rab32 knockdown reduced cell proliferation and cell size, together with increased nuclear localization of transcription factor EB (TFEB) and lysosome biogenesis. Mechanistically, Rab32 appeared to interact with mTOR kinase in a unique GTP-independent manner. Finally, by using biochemically isolated lysosome fractions, we demonstrated a reduction in the lysosome association of mTOR, regulatory-associated protein of mTOR (RPTOR, hereafter referred to as Raptor) and mTORC1 pathway proteins, such as RagC and Lamtor1, following knockdown of Rab32, suggesting that Rab32 functions to regulate mTOR trafficking to lysosomes. Together, these findings suggest that Rab32 acts as a novel regulator of cell metabolism and growth through the promotion of mTORC1 activity.

RESULTS
Rab32 localizes to late endosomes and lysosomes
Rab32 has been previously reported to localize to a number of metabolic organelles, such as the ER, mitochondria and lysosomes and/or autophagosomes in COS1 and COS7 and HeLa cells, as well as pigment granules in melanocytes (Alto et al., 2002; Bui et al., 2010; Hirota and Tanaka, 2009). To further define the role of Rab32 in more-differentiated epithelial cells, such as hepatocytes, we first sought to analyze its subcellular localization in both primary rat hepatocytes and Hep3B human hepatoma cells. As shown in Fig. 1, GFP-tagged wild-type (WT) Rab32 displayed a prominent localization around lysotracker-positive acidic vesicles, suggestive of late endosomes/lysosomes. Similar localization was observed with FLAG-tagged Rab32, and with Lamp2A- or Lamp1-labeled lysosomes in primary rat hepatocytes or Hep3B cells, respectively. Both WT and GTP-bound (Q85L) Rab32 forms exhibited similar late endosome and/or lysosome associations, whereas GDP-bound (T39N) Rab32 showed reduced localization to these organelles. In support of previous studies (Alto et al., 2002; Bui et al., 2010), Rab32 was also observed to localize to mitochondria and the ER in a subset of Hep3B cells, but this was rarely observed in primary rat hepatocytes (data not shown). Altogether, Rab32 distributes to various metabolic organelles but appears most prominent on acidic vesicles, such as late endosomes and lysosomes in hepatocytes.

Regulation of mTORC1 signaling, cell proliferation and cell size by Rab32
To gain a better understanding of the role that Rab32 has in epithelial cell function, we conducted an unbiased reverse phase protein array (RPPA) to screen for changes in protein signaling pathways involving cell growth, proliferation, metastasis, metabolism and apoptosis. Hep3B cells were subjected to control or Rab32 siRNA treatment for 72 h, followed by cell lysis, and analysis of changes in

the levels of total or phosphorylated protein by using a ∼220 antibody-based array (Chang et al., 2015). This assay revealed that several prominent signaling proteins related to the mTOR pathway are attenuated in response to Rab32 knockdown (Table S1). Included on this list are upstream regulators of mTORC1, such as phosphorylated Akt and proline-rich Akt substrate of 40 kDa (PRAS40, officially known as AKT1S1), mTOR itself as well as downstream mTORC1 targets, such as S6K (Fig. 2A) (Dibble and Cantley, 2015). To further assess the impact Rab32 depletion has on mTORC1 signaling, we analyzed the phosphorylation of the individual downstream mTORC1 substrates by western blot analysis. As shown in Fig. 2B, Rab32-depleted Hep3B cells exhibited a ∼50% decrease in the phosphorylation of the mTORC1 substrate S6K and its downstream substrate ribosomal protein S6. Interestingly, a significant impact on the phosphorylation of the mTORC1 substrate eukaryotic translation initiation factor 4E-binding protein 1 (EIF4EBP1, hereafter referred to as 4EBP1) was not observed relative to total 4EBP1 amounts in the Hep3B cell model (Fig. 2B). These effects were confirmed across four individual Rab32 siRNAs (Fig. S1). mTORC1 is also known to phosphorylate the autophagy regulator ULK1 at Ser757 (Kim et al., 2011). Phosphorylation of ULK1 at this residue appeared modestly reduced relative to total ULK1 following knockdown of Rab32 (Fig. 2B and Fig. S1). Similar inhibition of mTORC1 was also observed in HeLa cells upon Rab32 depletion (Fig. S2A). These results show that loss of Rab32 affects phosphorylation of mTORC1 substrates – with the most dramatic effects on S6K and S6.

S6K is known to regulate protein synthesis and cell size through phosphorylation of S6 as well as activate the transcription factor sterol regulatory element binding protein 1 (SREBF1, hereafter referred to as SREBP1) to express genes involved in fatty acid, triglyceride and cholesterol synthesis (Düvel et al., 2010; Owen et al., 2012). Given the impact of Rab32 on S6K activity described above, we assessed the activation of SREBP1 in control or Rab32-depleted cells as an additional downstream read-out of S6K activity. Indeed, as seen in the luciferase assay shown in Fig. 2C, transcription of the SREBP1 target promoter sequence of fatty acid synthase (FASN) was reduced by a significant 70% in Rab32-depleted cells.

As Rab32 appears to localize on lysosomes and play a role in the regulation of mTORC1 signaling, we further predicted that Rab32 depletion would impact cell proliferation and size – properties known to be physiologically driven by mTORC1. First, Hep3B cell proliferation and viability was diminished nearly 50% following Rab32 knockdown, as measured by a standard crystal violet assay compared to control cells (Fig. 2D). This finding was further confirmed by an alternative colorimetric MTS proliferation assay, which revealed a ∼40% loss in cell proliferation and/or viability after Rab32 depletion (Fig. 2E). Additionally, Rab32-depleted Hep3B and HeLa cells exhibited a dramatic decrease in the average 2D cell area on glass coverslips, and also in the average cell diameter of trypsinized cells in suspension compared to control cells (Fig. 2F,G and Fig. S2B,C). Collectively, these results indicate that loss of Rab32 decreases cell proliferation, viability and cell size, consistent with an attenuation of mTORC1 signaling.

Rab32 is essential for amino acid-induced mTORC1 activation
It is well-documented that amino acids are crucial for mTORC1 activation and signaling (Saxton and Sabatini, 2017). During periods of starvation when the supply of amino acids is low, mTORC1 is inactive and thought to reside primarily within the
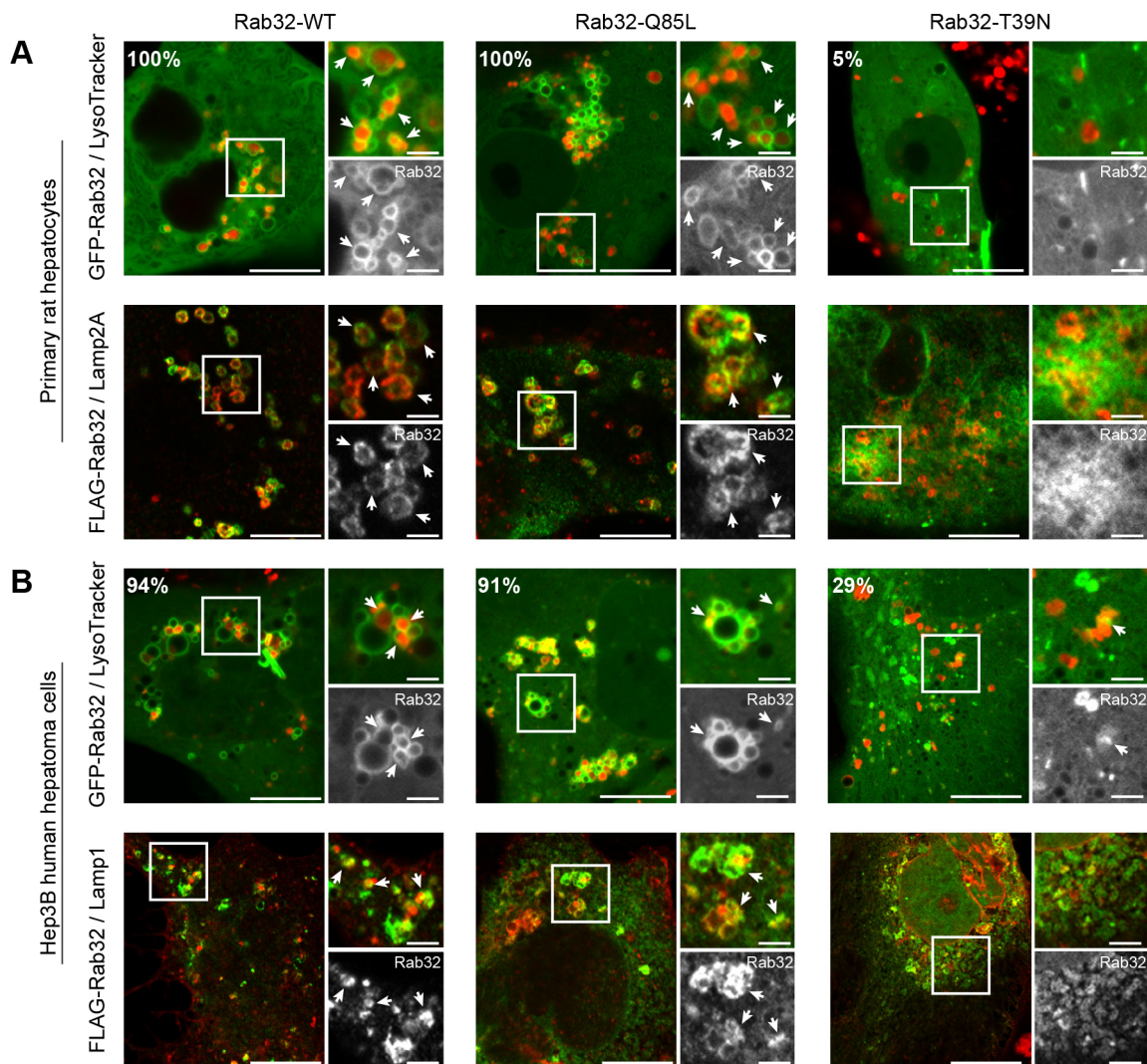
Fig. 1. Rab32 localizes to lysosomes. (A,B) Confocal images of live primary rat hepatocytes (A) or Hep3B human hepatoma hepatocytes (B) showing the different distributions of Rab32. First row in A and B show cells expressing GFP-tagged wild-type (WT) Rab32 (Rab32-WT), GTP-bound (Q85L) Rab32 (Rab32-Q85L) or GDP-bound (T39N) Rab32 (Rab32-T39N) (all green) co-labeled with Lysotracker Deep Red dye to stain acidic late endosomes/lysosomes (pseudocolored in red). In each top left corner the frequency of cells showing distribution of Rab32 to late endosomes/lysosomes is provided (in %); $n=20$ (WT), $n=22$ (Q85L), $n=20$ (T39N) cells for primary rat hepatocytes; $n=53$ (WT), $n=47$ (Q85L), $n=52$ (T39N) cells for Hep3B cells. Second row in A and B show cells expressing FLAG-tagged Rab32 proteins (green) co-stained for lysosomal marker Lamp2A or coexpressing Lamp1-mCherry (red). Arrows point to examples of Rab32 surrounding late endosomes/lysosomes. Boxed areas in main images are shown magnified in respective insets. Scale bars: 10 μm, insets 2 μm.

cytosol. However, upon amino acid replenishment, mTOR is rapidly recruited to the lysosomal surface by heterodimeric Rag GTPases – within a matter of minutes – where it becomes activated by Rheb GTPase (Sancak et al., 2010, 2008). To determine whether Rab32 is necessary for amino acid-induced activation of mTORC1, Rab32-depleted cells were starved in amino acid-free medium for 50 min followed by amino acid re-feeding for an additional 15 min. In cells treated with control siRNA, re-addition of amino acids resulted in a marked (10-fold) increase of mTORC1 activity, as assessed by phosphorylation of its downstream targets S6K and S6. However, in Rab32-depleted cells, phosphorylation of S6K was inhibited dramatically whereas phosphorylation of S6 was nearly abolished after amino acid re-addition (Fig. 3A,B). Phosphorylation of ULK1 was not significantly altered in Rab32-depleted Hep3B cells upon amino acid re-addition (Fig. 3A,B). These experiments produced similar findings in HeLa cells (Fig. S2D).

Because Rab32 knockdown appeared to diminish amino acid-induced mTORC1 activation, we predicted that overexpression of

Rab32 would potentiate mTORC1 signaling either in the presence or absence of amino acid manipulation. As seen in Fig. S3, overexpression of Rab32 WT, Q85L or T39N did not significantly increase mTORC1 signaling after stimulation with amino acids. Overall, these data suggest that Rab32 is necessary but not sufficient for mTORC1 activation following stimulation with amino acids.

In addition to stimulation with amino acids, mTORC1 can also be activated by cell culture serum supplemented with growth factors that activate the PI3K-Akt pathway (Manning et al., 2002; Menon et al., 2014). We therefore asked whether Rab32 participates in mTORC1 activation in response to serum and/or growth factor stimulation. To this end, cells were placed in serum-free HBSS for 1 h, then stimulated with 10% FBS-containing growth medium for 15 min and analyzed by western blotting. As seen in Fig. 3C,D, Rab32 depletion significantly inhibited phosphorylation of S6 but not of S6K or ULK1 relative to each protein in total. Overall, these data suggest that Rab32 regulates mTORC1 activity following stimulation with amino acids and, perhaps to a lesser extent, growth factors.
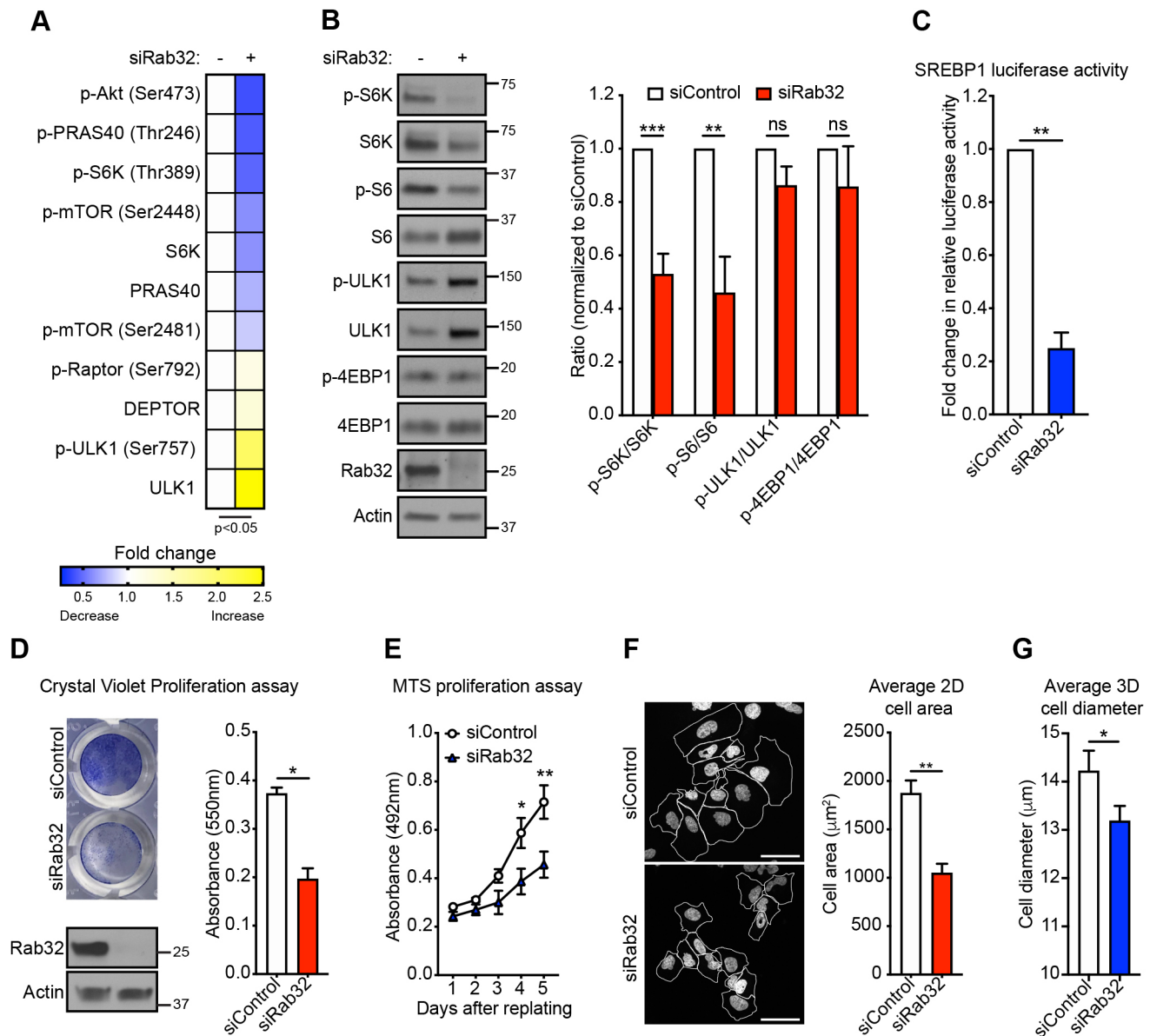
Fig. 2. The mTORC1 signaling pathway as well as cell proliferation and cell size are attenuated after Rab32 knockdown. (A) Heatmap of RPPA screen results, representing fold changes in mTOR pathway-related proteins after 72 h of Rab32 knockdown in Hep3B cells compared to control cells; blue shades represent fold changes <1 and yellow shades represent fold changes >1. Shown are significant changes determined by Student's t-test (P<0.05). (B) Western blot of Hep3B cells treated for 72 h with control siRNA (-) or Rab32 siRNA (+). Analyzed were specific downstream mTORC1 substrates in their phosphorylated (p-S6K, p-S6, p-ULK1, p-4EBP1) and unphosphorylated forms (S6K, S6, ULK1, 4EBP1), respectively. The bar graph represents fold changes in the phosphorylated versus total protein levels, consistent with RPPA findings. ns, not significant. (C) Bar graph representing relative SREBP1 transcriptional activity in control (siControl) or Rab32-depleted (siRab32) Hep3B cells that had been co-transfected with FASN firefly and internal control *Renilla* luciferase reporter constructs. FASN firefly luciferase values were normalized to control *Renilla* luciferase values for transfection efficiency. (D) Crystal Violet staining shows a ∼50% loss in Hep3B cell proliferation and viability, following 96 h treatment with Rab32 siRNA versus non-targeting control siRNA. Western blot shows the representative Rab32-knockdown efficiency in Hep3B cells. (E) Bar graph displays a significant decrease in Hep3B cell proliferation after Rab32 knockdown by cell proliferation (MTS) assay after 48 h of treatment with siRab32, followed by re-plating for 1-5 days, compared with siControl-treated cells. (F) Bar graph and representative images depict a ∼45% reduction in the average 2D cell area of Rab32 siRNA- versus control siRNA-treated Hep3B cells. Scale bars: 50 μm. (G) Bar graph shows the average 3D cell diameter of trypsinized control- or Rab32 siRNA-treated Hep3B cells. Data are presented as means±s.e.m. from n=3-4 independent experiments (B-G). Asterisks denote statistical significance by two-tailed paired Student's t-test (B-D,F,G) or 2-way ANOVA with Sidak post-hoc test (E) (*P<0.05, **P<0.01, ***P<0.001). Also see Figs S1 and S2A-C.

Loss of Rab32 increases nuclear TFEB localization and lysosome biogenesis

mTORC1 activity has been shown to play a critical inhibitory role in lysosome biogenesis through phosphorylation of transcription factor EB (TFEB), a key transcriptional regulator of numerous lysosomal and autophagy genes. As shown in several studies,

phosphorylation of TFEB by mTORC1 promotes TFEB retention in the cytoplasm, thereby preventing its transcriptional activity (Martina et al., 2012; Napolitano and Ballabio, 2016; Sardiello et al., 2009; Settembre et al., 2011). By contrast, inhibition of mTORC1 leads to TFEB dephosphorylation and translocation to the nucleus to promote transcription of genes related to lysosome
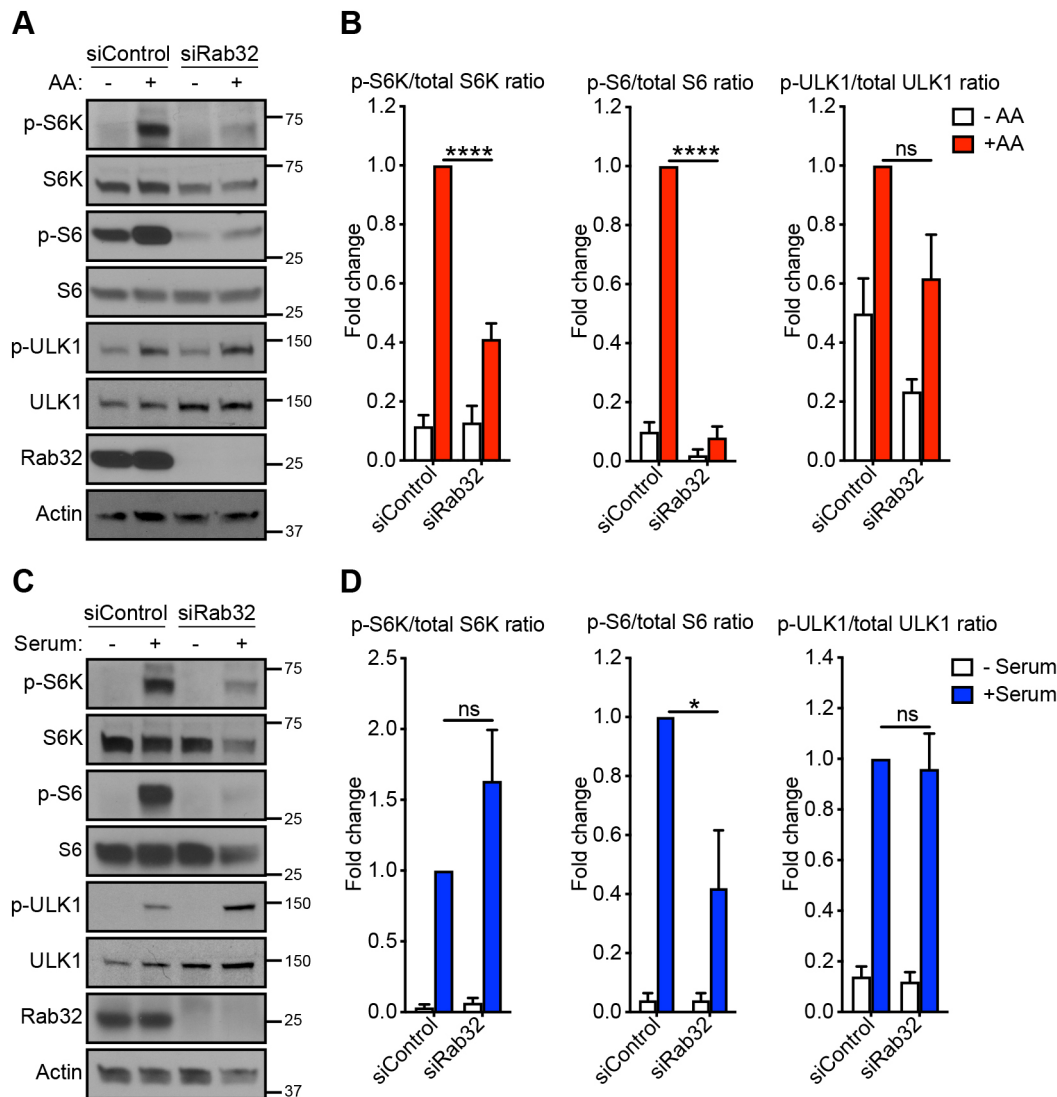
Fig. 3. Rab32 is required for robust amino acid-induced phosphorylation of S6K and S6 by mTORC1. (A,C) Representative western blots of Hep3B cells that had been treated with either siControl or siRab32 for 72 h. Cells in A were exposed to amino acid-depleted medium (-AA) for 50 min, then re-stimulated in amino acid-rich medium (+AA) for an additional 15 min. (B) Quantification of results shown in A, depicting a significant decrease in phosphorylated versus total S6K (p-S6K/total S6K ratio) and phosphorylated versus total S6 (p-S6/total S6 ratio) but not of phosphorylated versus total ULK1 (p-ULK1/total ULK1 ratio) after Rab32 knockdown. Cells in C were starved in serum-free HBSS for 1 h, then re-stimulated with medium containing 10% FBS for an additional 15 min. (D) Quantification of results shown in C depict a significant decrease in the ratio of p-S6/total S6 following serum stimulation, but not in those of p-S6K/total S6K or p-ULK1/total ULK1 after Rab32 knockdown. Fold changes are shown as means±s.e.m. of phosphorylated/total protein ratios from at least $n=5$ independent experiments. Asterisks denote statistical significance by two-tailed paired Student's t-test (*$P<0.05$, ****$P<0.0001$). Also see Figs S2D and S3.

biogenesis and autophagy (Roczniak-Ferguson et al., 2012; Settembre et al., 2012). Considering that Rab32 depletion inhibits mTORC1 activity, we predicted that this would also lead to increased nuclear TFEB, lysosome biogenesis and autophagy. To address this question, GFP-tagged TFEB was expressed in control and Rab32-depleted Hep3B and HeLa cells, and the percentage of cells with nuclear TFEB localization was quantified. Interestingly, a nearly 2-fold increase in the frequency of nuclear TFEB localization was observed following Rab32 knockdown (Fig. 4A-C and Fig. S4A), a result consistent with reduced mTORC1 activity in cells lacking Rab32.

To further assess the impact of Rab32 on lysosome biogenesis, the number and size of LysoTracker-stained lysosomes was measured together with the relative acidity of these vesicles by using the pH-sensitive LysoSensor dye. Consistent with an increase in nuclear TFEB localization, Rab32-depleted Hep3B cells exhibited an

increase in lysosome number per cell, with no significant effect on lysosome size or relative acidity (Fig. 4D,E). Western blot analysis showed that an increase in lysosome protein levels [Lamp1, Lamp2A and cathepsin D (CTSD)] was also observed following Rab32 knockdown (Fig. 4F,G). Rab32 knockdown in HeLa cells caused a significant increase in Lamp1 protein levels, although no significant effect was observed on lysosome number per cell area (Fig. S4B-E).

To confirm that Rab32 depletion did not affect lysosome function, we assessed the degradation of epidermal growth factor receptor (EGFR) following stimulation with its ligand, epidermal growth factor (EGF). As seen in Fig. 4H,I and Fig. S4F,G, Rab32 knockdown did not diminish EGFR degradation compared to controls in both Hep3B and HeLa cells. In fact, EGFR degradation was slightly accelerated in the absence of Rab32 at $t=60$ min in Hep3B cells (Fig. 4I). Overall, the above data further support the concept that loss of Rab32 inhibits mTORC1 signaling that, in turn,
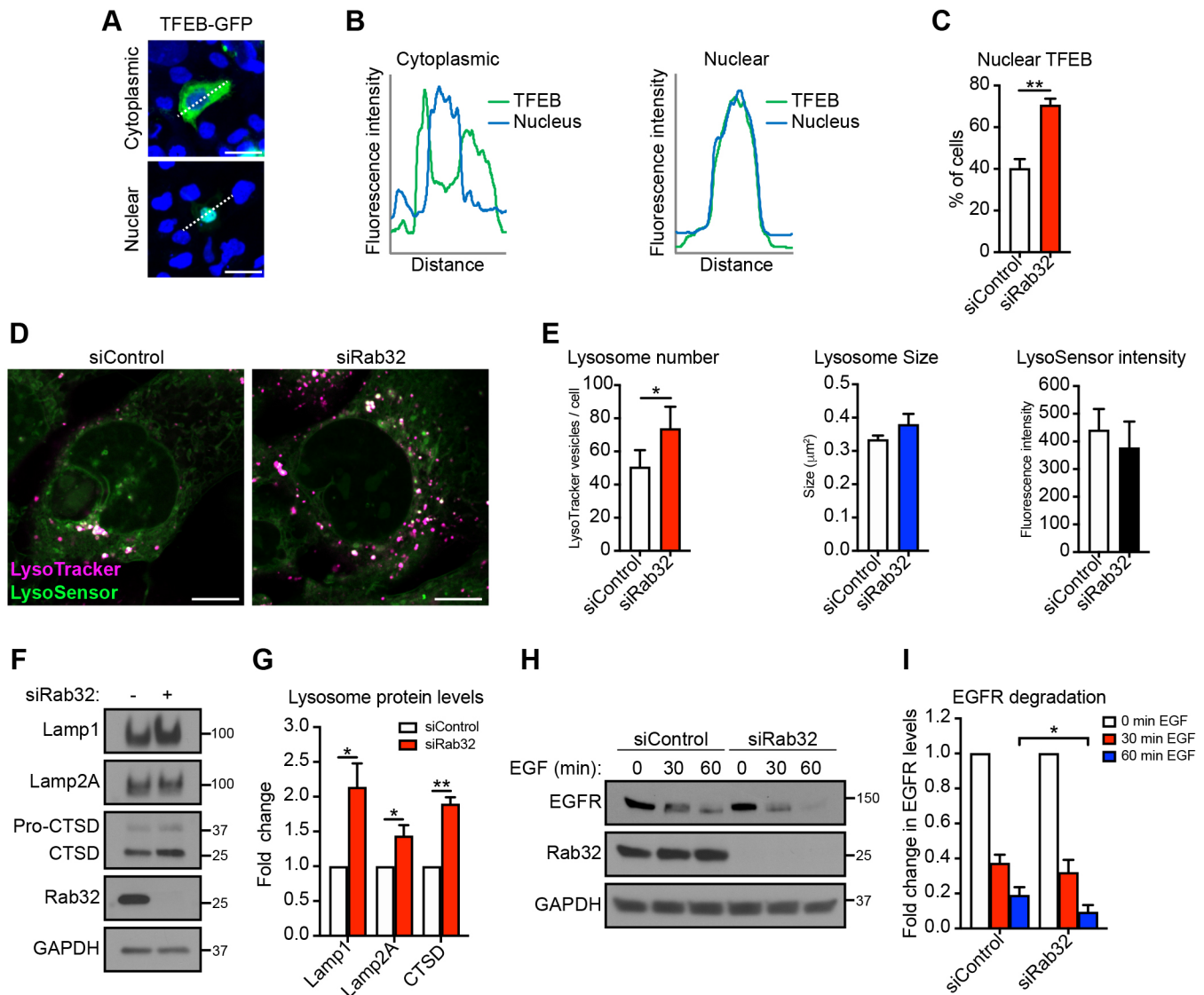
Fig. 4. Loss of Rab32 increases nuclear TFEB localization and lysosome biogenesis. (A) Representative images of cytoplasmic and nuclear TFEB-GFP localization in Hep3B cells. (B) Fluorescence line scans depict the nuclear versus cytoplasmic distribution of TFEB shown in A. (C) Bar graph displays a significant increase in the percentage of cells with nuclear TFEB-GFP localization after Rab32 knockdown in Hep3B cells. A total of n=785 and n=328 cells were counted for siControl and siRab32, respectively, from n=3 independent experiments. (D) Representative confocal images of Hep3B cells treated with the respective siRNAs and labeled with LysoTracker Deep Red (magenta) and LysoSensor (green) dyes, showing an increase in lysosome number following Rab32 knockdown. (E) Bar graphs depicting quantifications of results shown in D; a total of n=410 and n=386 cells were counted for siControl and siRab32, respectively, from n=4 independent experiments. (F) Western blot of Hep3B cells treated for 72 h with control (-) or Rab32 siRNA (+), and analyzed for changes in lysosomal protein levels of Lamp1, Lamp2A and cathepsin D (CTSD). (G) Bar graph representing fold changes in lysosomal proteins after Rab32 knockdown as analysed in F. (H) Western blot of Hep3B cells treated with respective siRNAs for 72 h and serum starved for 4 h in the presence of 50 µg/ml cycloheximide followed by treatment with 50 ng/ml EGF for the indicated time points and analyzed for EGFR degradation to test for lysosomal function. (I) Bar graph depicting the rate of EGFR degradation (normalized to GAPDH and to EGF treatment at t=0 min, for both siControl and siRab32). All data are presented as means±s.e.m. from n=3-4 independent experiments; asterisks denote statistical significance by two-tailed paired Student's t-test (*P<0.05, **P<0.01). Scale bars: 40 µm (A), 10 µm (D). Also see Fig. S4.

induces nuclear TFEB translocation and lysosome biogenesis. This effect appears to contrast the role of Rab32 in pigment-producing melanocytes, which show reduced biogenesis of the lysosome-related organelles (i.e. melanosomes) following Rab32 depletion.

Autophagy is reduced in Rab32-depleted cells

Inhibition of mTORC1 signaling is well known to activate autophagy to degrade cytosolic materials through lysosomal enzymes (Rabinowitz and White, 2010). On the basis of this, we predicted that this 'self-eating' process is enhanced following

Rab32 knockdown. To test the effect of Rab32 knockdown on autophagic flux, cells were treated with the lysosome inhibitor Bafilomycin A1 (BafA1, 100 nM, 2 h) to measure the relative increase in the accumulation of autophagosomes (increase in LC3-II levels) and the autophagy substrate p62 by western blot analysis. Under basal conditions (medium supplemented with 10% FBS) Rab32 knockdown modestly decreased LC3-II and p62 accumulation after treatment with BafA1, suggesting a perturbation in autophagic flux (Fig. 5A,B). In response to treatment with the potent mTOR inhibitor and autophagy activator Torin1 for 2 h, autophagic flux was
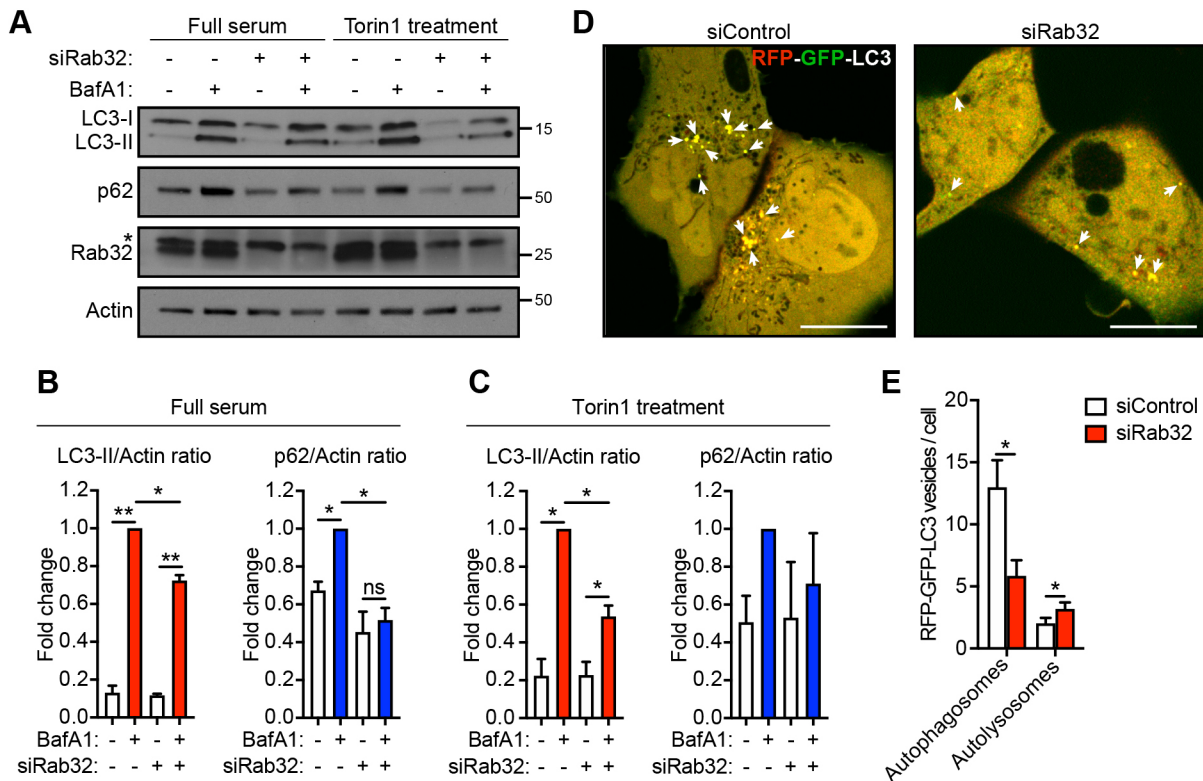
Fig. 5. Rab32 knockdown attenuates autophagy. (A) Western blot of Hep3B cells treated for 72 h with control or Rab32 siRNA followed by 2 h treatment with the lysosome inhibitor Bafilomycin A1 (BafA1, 100 nM) under basal, full serum conditions (10% FBS) or in the presence of the mTOR inhibitor Torin1 (1 μM) and analyzed for changes in the autophagic proteins LC3 and p62. The asterisk indicates a non-specific band. (B,C) Bar graphs representing fold changes of LC3-II and p62 protein levels (normalized to siControl+BafA1), indicating a reduction in autophagic flux. (D) Representative images of Hep3B cells expressing the RFP-GFP-LC3 tandem fluorescence reporter that had been treated with control or Rab32 siRNA for 72 h. RFP+/GFP+ fluorescence depicts autophagosomes (in yellow), whereas RFP+-only fluorescence depicts autolysosomes (in red). Arrows point to examples of RFP-GFP-LC3 puncta. (E) Bar graph representing the average number of autophagosome and autolysosome vesicles per cell from n=48 siControl and n=60 siRab32 treated cells from n=3 independent experiments. Data are presented as means±s.e.m. from n=3 independent experiments; asterisks denote statistical significance by two-tailed paired Student's t-test (*P<0.05, **P<0.01). Scale bars: 20 μm for siControl and 13 μm for siRab32. Also see Fig. S5.

similarly perturbed by Rab32 knockdown (Fig. 5A,C). The effect of Rab32 knockdown on autophagy was also measured using the RFP-GFP-LC3 fluorescence reporter. This probe indicates neutral-pH autophagosomes as yellow (combined RFP and GFP fluorescence). Upon autophagosome fusion with an acidic lysosome, the GFP fluorescence becomes quenched and appears as red-only puncta indicating a progression of the autophagic process. As seen in Fig. 5D,E, Rab32 knockdown caused a dramatic decrease in autophagosome number per cell (yellow puncta), with a modest increase in autolysosomes (red puncta) indicating that loss of Rab32 perturbs autophagosome formation. In HeLa cells, Rab32 knockdown caused an even more dramatic perturbation in autophagic flux, as assessed by western blot and fluorescence of the RFP-GFP-LC3 reporter (see Fig. S5). Together these data suggest that Rab32 knockdown perturbs autophagic flux, perhaps by attenuating autophagosome biogenesis. This result is surprising given that mTORC1 is inhibited following Rab32 knockdown but is nonetheless consistent with a previous study that suggests a role for Rab32 in autophagosome biogenesis (Hirota and Tanaka, 2009).

Rab32 interacts with mTOR kinase and regulates mTOR association with lysosomes

To gain a more detailed mechanistic understanding of mTORC1 regulation by Rab32, we assessed the subcellular localization of mTORC1 in relation to the lysosomal surface. Recent studies suggest that mTORC1 activation occurs at the lysosome in response to

nutrient signaling (Manifava et al., 2016; Sancak et al., 2010, 2008). Because Rab32 is present on lysosomes, we hypothesized that it colocalizes and associates with mTORC1 on these organelles. To test this, FLAG-tagged Rab32 was expressed in Hep3B cells together with GFP-tagged Lamp1 to label lysosomes; cells were then co-stained with an mTOR antibody. Notably, FLAG-Rab32 colocalized with endogenous mTOR on Lamp1-positive lysosomes in Hep3B cells, as shown in Fig. 6A. Additionally, colocalization between GFP-tagged Rab32, Lamp1-mCherry and mTOR was readily observed in primary rat hepatocytes (Fig. 6A). This result prompted us to test whether Rab32 associates with either mTOR kinase or any other mTOR complex components, using biochemical methods, such as GFP-Trap pulldown approach. Hep3B cells expressing GFP-Rab32 were lysed and incubated with GFP-binding agarose beads to pull down GFP vector control or GFP-tagged Rab32 and analyzed for binding to mTOR complex components. As depicted in Fig. 6B, pulldown of Rab32 revealed an association with mTOR as well as the mTORC1/2 subunit mLST8, but not with the mTORC1-specific subunit Raptor or the mTORC2-specific subunit rapamycin-insensitive companion of mammalian target of rapamycin (Rictor) under the conditions tested. Reciprocal coimmunoprecipitation of endogenous mTOR confirmed an interaction with FLAG-Rab32 together with the mTORC1/2 subunit mLST8 (Fig. 6C). To test whether this interaction is dependent upon the GTP-bound state of Rab32, we performed GST-Rab32 pulldown experiments using WT, Q85L and T39N Rab32 variants from Hep3B and HeLa cell lysates.
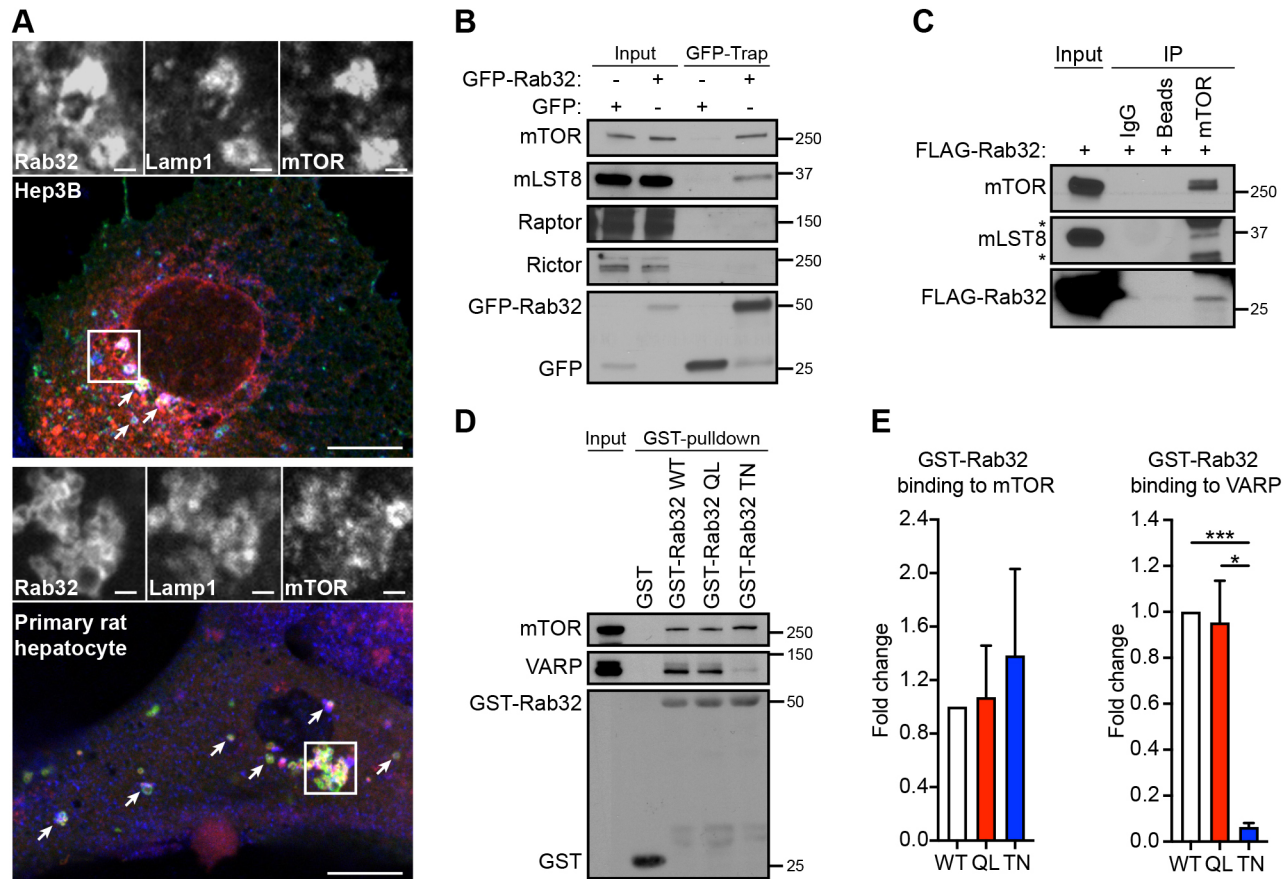
Fig. 6. Rab32 associates with mTOR. (A) Confocal images of Hep3B cells and primary rat hepatocytes show colocalization between Rab32, lysosomes and mTOR. Hep3B cells were co-transfected with FLAG-Rab32 (red), Lamp1-GFP (green) followed by staining for endogenous mTOR (blue). Primary rat hepatocytes were co-transfected with GFP-Rab32 (green), Lamp1-mCherry (red) and also stained for endogenous mTOR (blue). Arrows mark additional examples of colocalization. Scale bars: 10 μm, insets 1 μm. (B-E) Western blot analysis to test for an association between Rab32 mutants and select mTOR complex components. (B) Western blot analysis of Rab32 pulldowns from Hep3B cells that were transfected with either GFP vector or GFP-tagged Rab32 WT (GFP-Rab32) for 24 h followed by GFP-Trap pulldown and analyzed for binding to mTOR, mLST8, Raptor or Rictor (n=3 independent experiments). (C) Hep3B cells were transfected with FLAG-Rab32 WT for 24 h and subjected to coimmunoprecipitation with either IgG control antibody, beads alone or mTOR antibody, and analyzed for binding to FLAG-Rab32 (n=2 independent experiments). Asterisks mark non-specific bands. (D) GST-pulldown assay using purified Rab32 proteins (WT, Q85L or T39N) incubated with Hep3B cell lysates and analyzed for binding to mTOR and the Rab32 effector VARP (n=3 independent experiments). (E) Bar graphs depicting quantification of GST-Rab32 pulldown of mTOR or VARP from results shown in D (normalized to GST-Rab32 WT). Data are presented as means±s.e.m. Asterisks denote statistical significance by two-tailed paired Student's t-test (*P<0.05, ***P<0.001). Also see Fig. S6A,B.

The capacity of Rab32 to bind to a known effector (VARP) was used as a positive control (Tamura et al., 2009). Surprisingly, similar levels of endogenous mTOR were observed in pulldown assays using all the GST-Rab32 variants, whereas, as expected, only WT and QL Rab32 were associated with the effector VARP (Fig. 6D,E and Fig. S6A,B). Together, these findings suggest that Rab32 can associate with mTOR regardless of its nucleotide bound status.

As mTOR trafficking to lysosomes is crucial for its subsequent activation and signaling (Sancak et al., 2010), we reasoned that Rab32 may regulate mTOR association with lysosomes. To test this, lysosomes were biochemically isolated using an immunoprecipitation-based pulldown of the HA-tagged transmembrane lysosome protein TMEM192 as described previously (Abu-Remaileh et al., 2017). Hep3B cells were depleted of endogenous Rab32 using siRNA treatment and transfected with TMEM192-HA followed by cell homogenization and pulldown of intact lysosomes using magnetic anti-HA beads. Importantly, lysosome-associated mTOR levels were significantly reduced (∼50%) in Lamp1-enriched lysosome fractions gleaned from the Rab32-depleted cells compared to control cells (Fig. 7A,B). In addition, the mTORC1 subunits Raptor, RagC and

Lamtor1 were also present on lysosomes, although at levels that were lower than in control cells. Similar Lyso-IP results were observed in HeLa cells (Fig. S6C). Together, these data suggest that loss of Rab32 impairs mTORC1 association with lysosomes.

Given that Rab32 knockdown appears to inhibit mTORC1 signaling and lysosomal association, we reasoned that mTORC1 activity can be rescued by overexpression of active Rag heterodimers that drive mTORC1 to the lysosome (Sancak et al., 2010, 2008). As seen in Fig. 7C,D, expression of RagB^{GTP}/RagC^{GDP} heterodimers in Rab32-depleted Hep3B cells was sufficient to rescue phosphorylation of S6K and S6 to that of control levels after stimulation with amino acids (Fig. 7C,D). Similar effects were observed in HeLa cells (Fig. S6D,E). Overall, our data support a model whereby loss of Rab32 reduces lysosomal mTORC1 levels and thus attenuates mTORC1 activity (Fig. 7E).

DISCUSSION
In this study we report that Rab32 localizes to lysosomes (Fig. 1) and supports robust basal and amino acid-induced mTORC1 phosphorylation of S6K and S6 substrates (Figs 2 and 3, Figs S1,
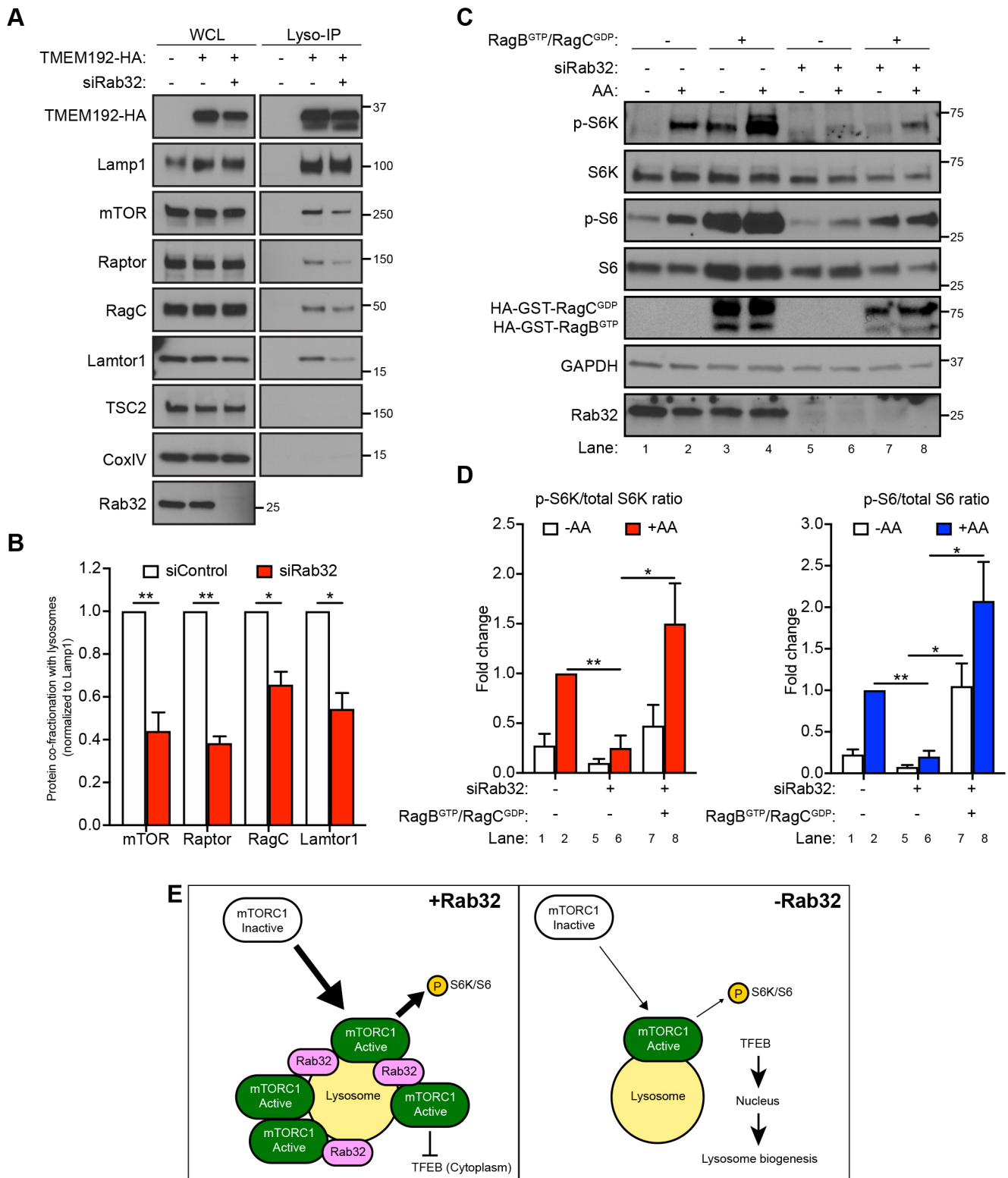
Fig. 7. See next page for legend.

S2). Loss of Rab32 inhibits mTORC1 signaling and reduces cell proliferation, viability and cell size (Fig. 2, Fig. S2). In agreement with mTORC1 inhibition, loss of Rab32 also promotes nuclear TFEB localization and lysosome biogenesis (Fig. 4, Fig. S4). We made two unexpected observations in this study. First, autophagy is also impaired in Rab32-depleted cells, perhaps due to reduced

autophagosome biogenesis (Fig. 5, Fig. S5). Second, Rab32 interacts with mTOR in a GTP/GDP-independent manner and promotes mTOR association with lysosomes (Figs 6 and 7, Fig. S6). Taken together, these findings highlight a novel role for the small GTPase Rab32 in regulating growth and metabolism of epithelial cells via the mTORC1 signaling pathway.

Fig. 7. Rab32 regulates mTORC1 association with lysosomes. (A) Representative western blot of biochemically-isolated lysosomes (Lyso-IP) from control or Rab32-knockdown Hep3B cells show the relative association of mTOR, Raptor, RagC and Lamtor1 with lysosomes. WCL, whole-cell lysate. (B) Bar graph shows the quantification of data shown in A. Protein levels were normalized to those of Lamp1 from Lyso-IP fractions (n=3-4 independent experiments). Data are presented as means±s.e.m. (C) Representative western blot of Hep3B cells that had been treated with either siControl or siRab32 for 72 h followed by expression of active Rag heterodimers (RagB^{GTP}/RagC^{GDP}) and subjected to 50 min amino acid starvation followed by 15 min re-stimulation with amino acids. (D) Quantification of results shown in C, depicting a significant decrease in phosphorylated versus total S6K (p-S6K/total S6K ratio) and phosphorylated versus total S6 (p-S6/total S6 ratio) after Rab32 knockdown, which is rescued by expression of active Rag heterodimers (n=4 independent experiments). Data are presented as means±s.e.m. (B,D) Asterisks denote statistical significance by two-tailed paired Student's t-test (*P<0.05, **P<0.01). Also see Fig. S6C-E. (E) Proposed model for Rab32 regulation of the mTORC1 signaling pathway. Rab32 facilitates mTORC1 association with lysosomes and promotes phosphorylation of downstream mTORC1 substrates (S6K/S6). However, loss of Rab32 decreases mTORC1 accumulation on lysosomes, thereby inhibiting mTORC1-mediated phosphorylation of S6K/S6 while promoting localization of TFEB to the nucleus and biogenesis of lysosomes.

The results presented here support a model whereby mTORC1 activity and association with lysosomes is dependent upon functional Rab32 (Fig. 7E). Indeed, other studies have demonstrated that activity of mTORC1 depends on its recruitment to lysosomes (by Rag GTPases), where it is subsequently activated (by Rheb GTPase) in response to nutrients and growth factors (Sancak et al., 2010, 2008). The finding that mTORC1 activity is restored in Rab32 knockdown cells upon overexpression of active Rag GTPases (Fig. 7C,D and Fig. S6D,E) is consistent with the premise that loss of Rab32 inhibits mTORC1 activation due to reduced mTORC1-lysosomal recruitment. It will be important to identify the binding motifs that enable binding between Rab32 and mTOR to better understand whether Rab32 directly regulates recruitment of mTOR and its attachment to the lysosome surface. It is worth noting that no differences were observed in the distribution of Rab32 to lysosomes in response to stimulation with amino acids – as was observed for mTORC1 (data not shown). Therefore, Rab32 might function as a 'docking site' for mTORC1 on the lysosomal surface or might affect the lysosomal proteome more generally. Indeed, Rab32 knockdown decreased lysosomal association of RagC and Lamtor1, which could also partially explain reduced lysosomal mTORC1 levels by Lyso-IP (Fig. 7A,B and Fig. S6C). Future studies will be required to assess how Rab32 depletion impacts on the lysosome proteome versus specific mTORC1-related components.

The effect of Rab32 manipulation on mTORC1 substrates

As described in Figs 2, 3 and Fig. S2, it was somewhat surprising to find that phosphorylation of S6K and S6 is strongly attenuated in the absence of Rab32, with little or no inhibition observed over phosphorylated ULK1 or 4EBP1 substrates, respectively. One possibility is that Rab32 regulates mTORC1 substrate specificity. However, it is perhaps more likely that different mTORC1 substrates (S6K, ULK1 and 4EBP1) exhibit different sensitivities to changes in mTORC1 kinase activity. For example, treatment with rapamycin was shown to readily inhibit S6K phosphorylation in most cell types, whereas phosphorylation of 4EBP1 was not affected (Choo et al., 2008; Qin et al., 2016). In line with this, Kang et al. identified that S6K is a weak mTORC1 substrate, whereas both ULK1 and 4EBP1 are phosphorylated with much higher affinity by mTORC1 (Kang et al., 2013). The authors proposed that the mTORC1 affinity to its substrate explains why treatment with

rapamycin inhibits phosphorylation of S6K, while mTORC1-mediated phosphorylation of ULK1 or 4EBP1 is not readily inhibited under the same conditions. Hence, the effect of Rab32 knockdown on S6K and S6 appears to mimic effects that are similar to those seen after treatment with rapamycin.

Rab32 binds to mTOR in a GTP/GDP-independent manner

The results presented here suggest that, whereas WT and GTP-bound Rab32 appear to localize to lysosomes at a higher frequency than the GDP-bound form (Fig. 1), the GTPase activity of Rab32 is not required for mTOR binding. The findings from the GST-pulldown experiments indicated that all Rab32 forms display equal binding capacity to endogenous mTOR, whereas the known Rab32 effector VARP only interacts with WT and GTP-bound forms (Fig. 6D,E and Fig. S6A,B). These observations suggest that Rab32 associates with mTOR kinase independent of its nucleotide-bound status, a contrast compared with many traditional Rab-effector interactions (Zhen and Stenmark, 2015). It should be noted, however, that some GTPase-independent functions have been described previously. For example, the Rho GTPase Rac1 acts independently of its GTPase activity as an adaptor protein for mTOR and regulates cellular membrane associations of both mTORC1 and mTORC2 complexes (Saci et al., 2011). Rab21 has also been implicated in binding to integrin receptors regardless of its GTP/GDP nucleotide status, whereas other Rab proteins, such as Rab27a and Rab11, have been reported to associate with interacting partners specifically in their GDP-bound states (Kimura et al., 2008; Mai et al., 2011; Shirane and Nakayama, 2006). Since the GDP-bound T39N form of Rab32 is not frequently observed at the lysosome surface, it is possible that it can interact with mTOR on different organelles. Indeed, both mTOR complexes and their substrates have been suggested to reside in additional organelles besides the lysosome (Betz and Hall, 2013; Betz et al., 2013; Thomas et al., 2014).

Regulation of lysosome biogenesis and autophagy by Rab32

Results from the current study suggest that Rab32 knockdown increases lysosome biogenesis, perhaps by inhibiting mTORC1. Indeed, loss of Rab32 increased nuclear localization of TFEB, lysosome numbers and lysosome protein levels, which is consistent with inhibition of mTORC1 signaling (Fig. 4, Fig. S4). This observation is interesting, given that Rab32 and its closest family member Rab38 have been previously reported to play tissue-specific and functionally redundant roles in the biogenesis of melanosomes (lysosome-related organelles) (Bultema et al., 2014; Tamura et al., 2009; Wasmeier et al., 2006). In fact, Rab32 and Rab38, and their effector VARP are crucial for cargo sorting during melanosome maturation, as disruption of Rab32, Rab38 or VARP activity causes mistrafficking of melanin-synthesizing enzymes as well as defective melanogenesis (Marks et al., 2013). Thus, whereas Rab32 knockdown in melanocytes inhibits melanosome biogenesis, Rab32 knockdown in other epithelial cells appears to promote lysosome biogenesis through inhibition of mTORC1.

As a master regulator of cell growth and metabolism, mTORC1 also integrates lysosomal nutrient sensing to monitor and balance anabolic and catabolic processes. Under nutrient-replete conditions, autophagy progression is inhibited due to phosphorylation of the ULK1 complex by mTORC1. However, attenuation of mTORC1 signaling during periods of nutrient starvation or stress can lead to autophagosome formation and autophagy activation (Kim et al., 2011; Rabanal-Ruiz et al., 2017). We were surprised to find that depletion of endogenous Rab32 perturbed autophagosome formation even though mTORC1

signaling was also inhibited (Fig. 5 and Fig. S5). However, the effect Rab32 knockdown has on ULK1 phosphorylation was modest compared to its effect on phosphorylation of S6K and S6. Thus, residual ULK1 phosphorylation by mTORC1 might contribute to autophagy inhibition in Rab32-depleted cells, especially given the apparent increase in total ULK1 protein levels (∼2.5-fold, data not shown). In addition, Rab32 might affect autophagosome biogenesis directly, consistent with previous studies (Hirota and Tanaka, 2009; Matsui and Fukuda, 2013). Similar effects on mTORC1 and autophagy have also been reported for other Rab GTPases. For example, Rab1A has been proposed to activate both mTORC1 signaling in response to amino acid signaling at the Golgi as well as the formation of autophagosome vesicles (Huang et al., 2011; Thomas et al., 2014; Winslow et al., 2010).

In summary, we have identified Rab32 as a lysosome component which acts as a novel regulator of cellular growth and metabolism through the regulation of mTORC1 signaling. Importantly, it appears that Rab32 is necessary for both basal and amino acid-induced activation of mTORC1 and phosphorylation of S6K and S6, as well as the regulation of nuclear TFEB localization and lysosome biogenesis. Supportive of these findings is that Rab32 interacts with mTOR kinase and facilitates mTOR association with lysosomes, which appears to be important for downstream mTORC1 signaling. Ultimately, it would be of interest to understand the physiological role of Rab32 regulation and perturbation of mTORC1, as they pertain to cellular metabolic processes, such as hepatic steatosis as well as regeneration and neoplastic growth.

MATERIALS AND METHODS
Antibodies, plasmids and reagents
Antibodies were used at 1:1000 for western blotting (WB) or 1:100 for immunofluorescence (IF) analysis unless otherwise specified. Antibodies against CoxIV (#4850), cathepsin D (#2284), EGFR (#2232), FLAG (#8146 for IF and #14793 for WB), GAPDH (#5174 at 1:5000), GβL/mLST8 (#3274), HA (#3724 at 1:10,000), Lamtor1 (#8975), LC3 (#2775), mTOR (#2983 at 1:200 for IF), p62 (#5114), p70 S6K (Thr389) (#9234), p70 S6K (#9202), RagC (#3360), Raptor (#2280), Rictor (#2114), S6 (Ser235/236) (#4858 at 1:5000), S6 (#2217 at 1:3000), TSC2 (#4308), ULK1 (Ser757) (#6888), ULK1 (#8054), 4EBP1 (Thr37/46) (#2855) and 4EBP1 (#9644) were from Cell Signaling (Danvers, MA). Antibodies against GFP (#sc-9996 at 1:2000), GST (#sc138 at 1:2000), Lamp1 (#sc-20011) and Rab32 (#sc-390206 at 1:500) were from Santa Cruz (Santa Cruz, CA). The anti-Raptor antibody (#42-4000) was from ThermoFisher (Rockford, IL). Antibodies against LAMP2A (#ab18528) and VARP (#108216) antibodies were from Abcam (San Francisco, CA). The anti-actin (#A2066 at 1:2000) antibody was from Sigma (St Louis, MO). For western blot analysis, HRP-conjugated goat anti-rabbit and anti-mouse antibodies (at 1:5000) were purchased from Invitrogen (Carlsbad, CA), which were detected using SuperSignal Pico or Femto substrates from ThermoFisher. The goat anti-rabbit and anti-mouse secondary antibodies conjugated to either Alexa-Fluor-488, Alexa-Fluor-594 or CY5 (at 1:500) and ProLong Antifade reagent used for IF staining were all obtained from ThermoFisher. Other reagents used were: LysoTracker Deep Red (#L12492) and LysoSensor Green DND-189 (#L7535) from ThermoFisher; Torin1 (#4247) from Tocris (Bristol, United Kingdom); Chaps (#220201) from EMD Millipore (Temecula, CA); all other reagents were obtained from Sigma unless otherwise specified.

siRNA oligonucleotides targeting human Rab32 (siGenome SMARTpool (#M-009920-02-0005) and individual oligonucleotides (#D-009920-01-0002, #D-009920-02-0002, #D-009920-03-0002, #D-009920-05-0002) or control non-targeting oligonucleotides were purchased from Dharmacon/Horizon Discovery Group (Lafayette, CO). siRab32 pool oligonucleotides were used throughout the paper unless otherwise specified.

The human WT, Q85L and T39N FLAG-Rab32 constructs were a kind gift from Dr John D. Scott (University of Washington, Seattle, WA). GFP-Rab32

constructs were cloned by amplifying Rab32 sequence from FLAG-Rab32 constructs using the following primers: 5′-ATGCCTCGAGTCATGGCGG-GCGGAG-3′ and 5′-GCATGAATTCGCTCAGCAACACTGGGATTTG-3′, followed by cloning into pEGFP-C1 vector (Clonetech, Palo Alto, CA) using XhoI and EcoRI enzymes (New England BioLabs, Ipswich, MA). GST-Rab32 constructs were cloned by amplifying Rab32 sequence from GFP-Rab32 constructs using the following primers: 5′-GGATCCATGGC-GGGCGGAGGAGCC-3′ and 5′-CTCGAGTCAGCAACACTGGGATTT-C-3′, followed by cloning into TA-pCR2.1 vector (Invitrogen) using BamHI and XhoI enzymes and subcloned into pGEX-4T-1 (GE Healthcare, Chicago, IL) using the same enzymes.

Plasmids obtained from Addgene (Watertown, MA): pLJC5-Tmem192-3xHA (#102930) (Abu-Remaileh et al., 2017), pRK5-HA GST RagBQ99L (RagB^GTP^) (#19303) and pRK5-HA GST-RagC75L (RagC^GDP^) (#19305) (Sancak et al., 2008) were a gift from David Sabatini; fatty acid synthase (FAS) promoter luciferase was a gift from Bruce Spiegelment (#8890) (Kim et al., 1998), RFP-EGFP-LC3 was a gift from Tamotsu Yoshimori (#21074) (Kimura et al., 2007), pEGFP-N1-TFEB was a gift from Shawn Ferguson (#38119) (Roczniak-Ferguson et al., 2012). pRL-TK *Renilla* control reporter vector (#E2241; Promega Madison, WI) was a kind gift from Dr Gregory J. Gores (Mayo Clinic, Rochester, MN). Lamp1 constructs were previously described (Schulze et al., 2013).

Cell culture and transfections
Primary rat hepatocyte isolation and culturing was performed as previously described (Schott et al., 2017). Hep3B2.1-7 (Hep3B), hepatocellular carcinoma from human liver (ATCC HB-8064, Manassas, VA), was maintained in minimum Eagle's medium (MEM) (Corning, Corning NY) with 10% fetal bovine serum (FBS), 100 U/ml penicillin, 100 μg/ml streptomycin (ThermoFisher) and supplemented with 1 mM sodium pyruvate, nonessential amino acids, and 0.075% (wt/vol) sodium bicarbonate (Corning). HeLa cell line, an adenocarcinoma from human cervix (ATCC CCL-2), was maintained in Dulbecco's modified Eagle's medium (Corning) with 10% FBS, 100 U/ml penicillin, and 100 μg/ml streptomycin. Cells are routinely tested for contamination. All cells were grown at 37°C in 5% CO_2 on acid-washed coverslips for fluorescence microscopy and in plastic culture dishes for biochemical analysis. Amino acid-free medium was formulated according to manufacturer's instructions (US Biological Life Sciences, Salem, MA; #D9800-13). To make amino acid-rich medium, amino acid-free medium was supplemented with MEM amino acids solution (Sigma; #M5550) and L-Glutamine (Gibco/ThermoFisher; #A2916801). For serum starvation and re-stimulation experiments we used Hanks' Balanced Salt Solution (HBSS) (Gibco; #24020117) followed by re-stimulation with 10% FBS MEM medium. Cells were transfected using Lipofectamine 2000 for DNA constructs or RNAiMAX for siRNA reagents (both from ThermoFisher) according to the manufacturer's protocol.

Fluorescence microscopy
Cells were processed for immunofluorescence as previously described (Henley and McNiven, 1996). In brief, cells were rinsed in PBS, fixed in 2.5% formaldehyde, permeabilized in 0.1% Triton X-100 for 2 min and blocked in buffer containing 5% goat serum. Fixed samples were then incubated with primary and secondary antibodies diluted in blocking buffer at 37°C. For images of live cells, cells were plated on glass-bottomed imaging dishes (Cell E&G LLC, San Diego, CA) following transfection and maintained at 37°C and 5% CO_2 for the duration of imaging. LysoTracker and LysoSensor staining was performed according to manufacturer's protocol. Images of both fixed and live cells were acquired using Zeiss LSM 780 confocal microscope (Carl Zeiss, Oberkochen, Germany). Images of TFEB-GFP localization were acquired using a Zeiss AxioObserver epifluorescence microscope (Carl Zeiss, Thornwood, NY) equipped with a Colibri 7 LED light source. Image analysis was assessed using ImageJ software (NIH).

Coimmunoprecipitation experiments
For immunoprecipitation of GFP-tagged proteins, GFP-Trap agarose beads (Chromotek, Planegg-Martinsried, Germany) were used following manufacturer's protocol. For immunoprecipitation of endogenous mTOR, cells were collected in 0.3% CHAPS lysis buffer (40 mM HEPES pH 7.4,

120 mM NaCl, 1 mM EDTA, 10 mM Pyrophosphate, 10 mM glycerophosphate, 0.3% CHAPS) containing complete protease (Roche, Basel, Switzerland) and Halt phosphatase (ThermoFisher; #78440) inhibitors, lysed on ice for 30 min and centrifuged to remove nuclei and cell debris. Protein concentrations were determined by BCA assay (Pierce/ThermoFisher; #23225). Cell lysates were precleared with prewashed Protein A-Sepharose or Protein G PLUS-Agarose beads (Sigma, #P3391 or Santa Cruz, #sc-2002, respectively) and incubated with primary antibody against mTOR (Bethyl Laboratories, Montgomery, TX; #A301-143A), IgG control or beads alone as an additional control. The samples were then incubated with beads followed by four to six washes in lysis buffer (increased salt concentration to 150 mM NaCl). All protein samples subjected to western blot analysis were resolved by SDS-PAGE and transferred onto PVDF membrane (EMD Millipore; #IPVH00010), following immunoblotting and detection using autoradiography film (HyBlot CL from Denville Scientific, Holliston, MA) and Kodak X-OMAT automatic processor (Rochester, NY).

GST-Rab32 protein purification and pulldown
GST-fusion proteins were expressed in *Escherichia coli* BL21(DE3) pLysS-competent cells (Invitrogen) and purified using glutathione-coated beads (GE Healthcare) according to manufacturer's instructions. Cells were lysed in lysis buffer [6:1 ratio of TCMN100 buffer (20 mM Tris pH 7.4, 1 mM $CaCl_2$, 1 mM $MgCl_2$, 100 mM NaCl) and NTCMN300 buffer (0.5% NP40, 20 mM Tris pH 7.4, 1 mM $CaCl_2$, 1 mM $MgCl_2$ and 300 mM NaCl)] and incubated with GST-proteins for 1.5 h followed by four washes in NTCMN300 buffer.

Lysosome immunoprecipitation
Lysosomes were isolated as previously described with minor modifications (Abu-Remaileh et al., 2017). Briefly, cells were transfected with control or Rab32 siRNA followed by expression of TMEM192-HA lysosomal protein. Cells seeded into three 15 cm plates (∼80% confluency) were used for each Lyso-IP pulldown. Cells were washed twice with PBS (Corning; #21-040-CV), scraped in 1 ml of KPBS buffer (136 mM KCl, 10 mM KH_2PO_4, 2 mM EDTA pH 7.25) containing protease inhibitors and centrifuged at 1000 *g* for 2 min at 4°C. Pelleted cells were resuspended in 350 µl of KBPS and homogenized with 30-50 strokes in a 2 ml homogenizer. The homogenate was centrifuged again at 1000 *g* for 2 min and equal amounts of supernatant were incubated with 20 µl of prewashed anti-HA magnetic beads (ThermoFisher; #88837) on a rotor for 30 min at 4°C to pulldown HA-tagged lysosomes. Isolated lysosomes were then washed five times in KBPS buffer followed by two gentle washes on the vortex. Samples were boiled at 100°C for 5 min and subjected to SDS-PAGE western blot analysis.

EGFR degradation assay
Cells were incubated in serum-free medium for 4 h followed by stimulation with 50 ng/ml of EGF for 0, 30 or 60 min prior to cell lysis and western blot analysis. The treatments were performed in the presence of 50 µg/ml cycloheximide throughout the duration of experiment.

RPPA analysis
Reverse phase protein array (RPPA) assay was performed by the Antibody-Based Proteomics Core located in Baylor College of Medicine, Houston, TX as previously described (Chang et al., 2015). Briefly, Hep3B cells were transfected with either control or Rab32 siRNA for 72 h and reseeded at 70-80% confluency on 10 cm plates in quadruplicates. Cells were lysed in 150 µl of Tissue Protein Extraction Reagent (TPER) (Pierce; #7850) with 150 mM of NaCl and protease and phosphatase inhibitors (Roche; #11836153001 and #04906837001, respectively). Protein concentration was measured using BCA assay and 0.5 mg/ml of protein samples were denatured in 4XSDS sample buffer and boiled at 100°C for 8 min. Lysates were then shipped on dry ice for RPPA analysis to Baylor College of Medicine. We determined significant changes between control and Rab32 knockdown samples using Student's *t*-test (with $P<0.05$ considered to be significant).

Proliferation and cell size measurements
Cell proliferation and viability was determined using a standard crystal violet assay. In brief, cells were plated in 96-well plates at 4000 cells per well followed by siRNA knockdown for 96 h. Cells were then fixed in 25% glutaraldehyde and stained with crystal violet dye. Crystal violet staining was solubilized in 100 nM sodium citrate solution and measured at 550 nM wavelength using a plate reader. Colorimetric proliferation and viability assay of control and Rab32-depleted cells was performed using CellTiter 96 AQ_{ueous} Non-Radioactive Cell Proliferation Assay (MTS) kit following manufacturer's protocol (Promega; #G5421). The average 2D cell area was measured using cytosolic marker staining for reference using ImageJ software. The average 3D cell diameter of trypsinized cells in suspension was measured using a Countess automated cell counter (ThermoFisher).

Luciferase assay
Cells were subjected to siRNA knockdown for 24 h followed by co-transfection with FASN firefly and control pRL-TK *Renilla* luciferase vectors for additional 24 h. After re-seeding on 24-well plates, cells were then harvested in passive lysis buffer and assayed using Dual-Luciferase Reporter Assay System reagents (Promega; #E1910) using Synergy H1 Hybrid Multi-Mode Reader (BioTek, Vinooski, VT). Control *Renilla* luciferase vector values were used as an internal control to normalize transfection efficiency.

Statistical analysis and replication of experiments
Data are represented as mean ±s.e.m.; two-tailed paired Student's *t*-test was used to assess the statistical significance between two conditions (unless otherwise specified) with $P<0.05$ considered to be significant. Experiments were repeated at least three times and representative data are shown.

Competing interests
The authors declare no competing or financial interests.

Author contributions
Conceptualization: K.D.-M., M.B.S., M.A.M.; Methodology: K.D.-M., J.C., H.C., M.B.S.; Validation: K.D.-M., M.B.S.; Formal analysis: K.D.-M., M.B.S.; Investigation: K.D.-M., J.C., M.B.S.; Writing - original draft: K.D.-M.; Writing - review & editing: K.D.-M., M.B.S., M.A.M.; Visualization: K.D.-M.; Supervision: K.D.-M., M.B.S., M.A.M.; Project administration: K.D.-M., M.B.S., M.A.M.; Funding acquisition: K.D.-M., M.B.S., M.A.M.

Supplementary information
Supplementary information available online at
http://jcs.biologists.org/lookup/doi/10.1242/jcs.236661.supplemental

References
Abu-Remaileh, M., Wyant, G. A., Kim, C., Laqtom, N. N., Abbasi, M., Chan, S. H., Freinkman, E. and Sabatini, D. M. (2017). Lysosomal metabolomics reveals V-ATPase- and mTOR-dependent regulation of amino acid efflux from lysosomes. *Science* **358**, 807-813. doi:10.1126/science.aan6298

Alto, N. M., Soderling, J. and Scott, J. D. (2002). Rab32 is an A-kinase anchoring protein and participates in mitochondrial dynamics. *J. Cell Biol.* **158**, 659-668. doi:10.1083/jcb.200204081

Betz, C. and Hall, M. N. (2013). Where is mTOR and what is it doing there? *J. Cell Biol.* **203**, 563-574. doi:10.1083/jcb.201306041

Betz, C., Stracka, D., Prescianotto-Baschong, C., Frieden, M., Demaurex, N. and Hall, M. N. (2013). Feature Article: mTOR complex 2-Akt signaling at mitochondria-associated endoplasmic reticulum membranes (MAM) regulates mitochondrial physiology. *Proc. Natl. Acad. Sci. USA* **110**, 12526-12534. doi:10.1073/pnas.1302455110

Bui, M., Gilady, S. Y., Fitzsimmons, R. E. B., Benson, M. D., Lynes, E. M., Gesson, K., Alto, N. M., Strack, S., Scott, J. D. and Simmen, T. (2010). Rab32 modulates apoptosis onset and mitochondria-associated membrane (MAM) properties. *J. Biol. Chem.* **285**, 31590-31602. doi:10.1074/jbc.M110.101584

Bultema, J. J., Boyle, J. A., Malenke, P. B., Martin, F. E., Dell'Angelica, E. C., Cheney, R. E. and Di Pietro, S. M. (2014). Myosin vc interacts with Rab32 and Rab38 proteins and works in the biogenesis and secretion of melanosomes. *J. Biol. Chem.* **289**, 33513-33528. doi:10.1074/jbc.M114.578948

Chang, C.-H., Zhang, M., Rajapakshe, K., Coarfa, C., Edwards, D., Huang, S. and Rosen, J. M. (2015). Mammary stem cells and tumor-initiating cells are more resistant to apoptosis and exhibit increased DNA repair activity in response to DNA damage. *Stem Cell Reports* **5**, 378-391. doi:10.1016/j.stemcr.2015.07.009

Choo, A. Y., Yoon, S.-O., Kim, S. G., Roux, P. P. and Blenis, J. (2008). Rapamycin differentially inhibits S6Ks and 4E-BP1 to mediate cell-type-specific repression of mRNA translation. *Proc. Natl. Acad. Sci. USA* **105**, 17414-17419. doi:10.1073/pnas.0809136105

Dibble, C. C. and Cantley, L. C. (2015). Regulation of mTORC1 by PI3K signaling. *Trends Cell Biol.* **25**, 545-555. doi:10.1016/j.tcb.2015.06.002

Düvel, K., Yecies, J. L., Menon, S., Raman, P., Lipovsky, A. I., Souza, A. L., Triantafellow, E., Ma, Q., Gorski, R., Cleaver, S. et al. (2010). Activation of a metabolic gene regulatory network downstream of mTOR complex 1. *Mol. Cell* **39**, 171-183. doi:10.1016/j.molcel.2010.06.022

Fausto, N., Campbell, J. S. and Riehle, K. J. (2006). Liver regeneration. *Hepatology* **43**, S45-S53. doi:10.1002/hep.20969

Flinn, R. J., Yan, Y., Goswami, S., Parker, P. J. and Backer, J. M. (2010). The late endosome is essential for mTORC1 signaling. *Mol. Biol. Cell* **21**, 833-841. doi:10.1091/mbc.e09-09-0756

Fouraschen, S. M. G., de Ruiter, P. E., Kwekkeboom, J., de Bruin, R. W., Kazemier, G., Metselaar, H. J., Tilanus, H. W., van der Laan, L. J. and de Jonge, J. (2013). mTOR signaling in liver regeneration: Rapamycin combined with growth factor treatment. *World J. Transplant* **3**, 36-47. doi:10.5500/wjt.v3.i3. 36

Henley, J. R. and McNiven, M. A. (1996). Association of a dynamin-like protein with the Golgi apparatus in mammalian cells. *J. Cell Biol.* **133**, 761-775. doi:10.1083/jcb.133.4.761

Hirota, Y. and Tanaka, Y. (2009). A small GTPase, human Rab32, is required for the formation of autophagic vacuoles under basal conditions. *Cell. Mol. Life Sci.* **66**, 2913-2932. doi:10.1007/s00018-009-0080-9

Huang, J., Birmingham, C. L., Shahnazari, S., Shiu, J., Zheng, Y. T., Smith, A. C., Campellone, K. G., Heo, W. D., Gruenheid, S., Meyer, T. et al. (2011). Antibacterial autophagy occurs at PI(3)P-enriched domains of the endoplasmic reticulum and requires Rab1 GTPase. *Autophagy* **7**, 17-26. doi:10.4161/auto.7.1. 13840

Kang, S. A., Pacold, M. E., Cervantes, C. L., Lim, D., Lou, H. J., Ottina, K., Gray, N. S., Turk, B. E., Yaffe, M. B. and Sabatini, D. M. (2013). mTORC1 phosphorylation sites encode their sensitivity to starvation and rapamycin. *Science* **341**, 1236566. doi:10.1126/science.1236566

Kim, J. and Guan, K.-L. (2019). mTOR as a central hub of nutrient signalling and cell growth. *Nat. Cell Biol.* **21**, 63-71. doi:10.1038/s41556-018-0205-1

Kim, J. B., Sarraf, P., Wright, M., Yao, K. M., Mueller, E., Solanes, G., Lowell, B. B. and Spiegelman, B. M. (1998). Nutritional and insulin regulation of fatty acid synthetase and leptin gene expression through ADD1/SREBP1. *J. Clin. Invest.* **101**, 1-9. doi:10.1172/JCI1411

Kim, J., Kundu, M., Viollet, B. and Guan, K.-L. (2011). AMPK and mTOR regulate autophagy through direct phosphorylation of Ulk1. *Nat. Cell Biol.* **13**, 132-141. doi:10.1038/ncb2152

Kimura, S., Noda, T. and Yoshimori, T. (2007). Dissection of the autophagosome maturation process by a novel reporter protein, tandem fluorescent-tagged LC3. *Autophagy* **3**, 452-460. doi:10.4161/auto.4451

Kimura, T., Kaneko, Y., Yamada, S., Ishihara, H., Senda, T., Iwamatsu, A. and Niki, I. (2008). The GDP-dependent Rab27a effector coronin 3 controls endocytosis of secretory membrane in insulin-secreting cell lines. *J. Cell Sci.* **121**, 3092-3098. doi:10.1242/jcs.030544

Laplante, M. and Sabatini, D. M. (2012). mTOR signaling in growth control and disease. *Cell* **149**, 274-293. doi:10.1016/j.cell.2012.03.017

Li, G. (2011). Rab GTPases, membrane trafficking and diseases. *Curr. Drug Targets* **12**, 1188-1193. doi:10.2174/138945011795906561

Li, L., Kim, E., Yuan, H., Inoki, K., Goraksha-Hicks, P., Schiesher, R. L., Neufeld, T. P. and Guan, K.-L. (2010). Regulation of mTORC1 by the Rab and Arf GTPases. *J. Biol. Chem.* **285**, 19705-19709. doi:10.1074/jbc.C110.102483

Li, Q., Wang, J., Wan, Y. and Chen, D. (2016a). Depletion of Rab32 decreases intracellular lipid accumulation and induces lipolysis through enhancing ATGL expression in hepatocytes. *Biochem. Biophys. Res. Commun.* **471**, 492-496. doi:10.1016/j.bbrc.2016.02.047

Li, Z., Schulze, R. J., Weller, S. G., Krueger, E. W., Schott, M. B., Zhang, X., Casey, C. A., Liu, J., Stöckli, J., James, D. E. et al. (2016b). A novel Rab10-EHBP1-EHD2 complex essential for the autophagic engulfment of lipid droplets. *Sci. Adv.* **2**, e1601470. doi:10.1126/sciadv.1601470

Mai, A., Veltel, S., Pellinen, T., Padzik, A., Coffey, E., Marjomäki, V. and Ivaska, J. (2011). Competitive binding of Rab21 and p120RasGAP to integrins regulates receptor traffic and migration. *J. Cell Biol.* **194**, 291-306. doi:10.1083/jcb. 201012126

Manifava, M., Smith, M., Rotondo, S., Walker, S., Niewczas, I., Zoncu, R., Clark, J. and Ktistakis, N. T. (2016). Dynamics of mTORC1 activation in response to amino acids. *Elife* **5**, e19960. doi:10.7554/eLife.19960.024

Manning, B. D., Tee, A. R., Logsdon, M. N., Blenis, J. and Cantley, L. C. (2002). Identification of the tuberous sclerosis complex-2 tumor suppressor gene product tuberin as a target of the phosphoinositide 3-kinase/akt pathway. *Mol. Cell* **10**, 151-162. doi:10.1016/S1097-2765(02)00568-3

Marks, M. S., Heijnen, H. F. G. and Raposo, G. (2013). Lysosome-related organelles: unusual compartments become mainstream. *Curr. Opin. Cell Biol.* **25**, 495-505. doi:10.1016/j.ceb.2013.04.008

Martina, J. A., Chen, Y., Gucek, M. and Puertollano, R. (2012). MTORC1 functions as a transcriptional regulator of autophagy by preventing nuclear transport of TFEB. *Autophagy* **8**, 903-914. doi:10.4161/auto.19653

Matsui, T. and Fukuda, M. (2013). Rab12 regulates mTORC1 activity and autophagy through controlling the degradation of amino-acid transporter PAT4. *EMBO Rep.* **14**, 450-457. doi:10.1038/embor.2013.32

Matter, M. S., Decaens, T., Andersen, J. B. and Thorgeirsson, S. S. (2014). Targeting the mTOR pathway in hepatocellular carcinoma: current state and future trends. *J. Hepatol.* **60**, 855-865. doi:10.1016/j.jhep.2013.11.031

Menon, S., Dibble, C. C., Talbott, G., Hoxhaj, G., Valvezan, A. J., Takahashi, H., Cantley, L. C. and Manning, B. D. (2014). Spatial control of the TSC complex integrates insulin and nutrient regulation of mTORC1 at the lysosome. *Cell* **156**, 771-785. doi:10.1016/j.cell.2013.11.049

Napolitano, G. and Ballabio, A. (2016). TFEB at a glance. *J. Cell Sci.* **129**, 2475-2481. doi:10.1242/jcs.146365

Owen, J. L., Zhang, Y., Bae, S.-H., Farooqi, M. S., Liang, G., Hammer, R. E., Goldstein, J. L. and Brown, M. S. (2012). Insulin stimulation of SREBP-1c processing in transgenic rat hepatocytes requires p70 S6-kinase. *Proc. Natl. Acad. Sci. USA* **109**, 16184-16189. doi:10.1073/pnas.1213343109

Qin, X., Jiang, B. and Zhang, Y. (2016). 4E-BP1, a multifactor regulated multifunctional protein. *Cell Cycle* **15**, 781-786. doi:10.1080/15384101.2016. 1151581

Rabanal-Ruiz, Y., Otten, E. G. and Korolchuk, V. I. (2017). mTORC1 as the main gateway to autophagy. *Essays Biochem.* **61**, 565-584. doi:10.1042/EBC20170027

Rabinowitz, J. D. and White, E. (2010). Autophagy and metabolism. *Science* **330**, 1344-1348. doi:10.1126/science.1193497

Roczniak-Ferguson, A., Petit, C. S., Froehlich, F., Qian, S., Ky, J., Angarola, B., Walther, T. C. and Ferguson, S. M. (2012). The transcription factor TFEB links mTORC1 signaling to transcriptional control of lysosome homeostasis. *Sci. Signal.* **5**, ra42. doi:10.1126/scisignal.2002790

Saci, A., Cantley, L. C. and Carpenter, C. L. (2011). Rac1 regulates the activity of mTORC1 and mTORC2 and controls cellular size. *Mol. Cell* **42**, 50-61. doi:10. 1016/j.molcel.2011.03.017

Sancak, Y., Peterson, T. R., Shaul, Y. D., Lindquist, R. A., Thoreen, C. C., Bar-Peled, L. and Sabatini, D. M. (2008). The Rag GTPases bind raptor and mediate amino acid signaling to mTORC1. *Science* **320**, 1496-1501. doi:10.1126/science. 1157535

Sancak, Y., Bar-Peled, L., Zoncu, R., Markhard, A. L., Nada, S. and Sabatini, D. M. (2010). Ragulator-Rag complex targets mTORC1 to the lysosomal surface and is necessary for its activation by amino acids. *Cell* **141**, 290-303. doi:10.1016/j.cell.2010.02.024

Sardiello, M., Palmieri, M., di Ronza, A., Medina, D. L., Valenza, M., Gennarino, V. A., Di Malta, C., Donaudy, F., Embrione, V., Polishchuk, R. S. et al. (2009). A gene network regulating lysosomal biogenesis and function. *Science* **325**, 473-477. doi:10.1126/science.1174447

Saxton, R. A. and Sabatini, D. M. (2017). mTOR signaling in growth, metabolism, and disease. *Cell* **169**, 361-371. doi:10.1016/j.cell.2017.03.035

Schott, M. B., Rasineni, K., Weller, S. G., Schulze, R. J., Sletten, A. C., Casey, C. A. and McNiven, M. A. (2017). β-Adrenergic induction of lipolysis in hepatocytes is inhibited by ethanol exposure. *J. Biol. Chem.* **292**, 11815-11828. doi:10.1074/jbc.M117.777748

Schroeder, B., Schulze, R. J., Weller, S. G., Sletten, A. C., Casey, C. A. and McNiven, M. A. (2015). The small GTPase Rab7 as a central regulator of hepatocellular lipophagy. *Hepatology* **61**, 1896-1907. doi:10.1002/hep.27667

Schulze, R. J., Weller, S. G., Schroeder, B., Krueger, E. W., Chi, S., Casey, C. A. and McNiven, M. A. (2013). Lipid droplet breakdown requires dynamin 2 for vesiculation of autolysosomal tubules in hepatocytes. *J. Cell Biol.* **203**, 315-326. doi:10.1083/jcb.201306140

Schulze, R. J., Drižyte, K., Casey, C. A. and McNiven, M. A. (2017a). Hepatic Lipophagy: New Insights into Autophagic Catabolism of Lipid Droplets in the Liver. *Hepatol. Commun.* **1**, 359-369. doi:10.1002/hep4.1056

Schulze, R. J., Rasineni, K., Weller, S. G., Schott, M. B., Schroeder, B., Casey, C. A. and McNiven, M. A. (2017b). Ethanol exposure inhibits hepatocyte lipophagy by inactivating the small guanosine triphosphatase Rab7. *Hepatol. Commun.* **1**, 140-152. doi:10.1002/hep4.1021

Schulze, R. J., Schott, M. B., Casey, C. A., Tuma, P. L. and McNiven, M. A. (2019). The cell biology of the hepatocyte: a membrane trafficking machine. *J. Cell Biol.* **218**, 2096-2112. doi:10.1083/jcb.201903090

Sengupta, S., Peterson, T. R., Laplante, M., Oh, S. and Sabatini, D. M. (2010). mTORC1 controls fasting-induced ketogenesis and its modulation by ageing. *Nature* **468**, 1100-1104. doi:10.1038/nature09584

Settembre, C., Di Malta, C., Polito, V. A., Arencibia, M. G., Vetrini, F., Erdin, S., Erdin, S. U., Huynh, T., Medina, D., Colella, P. et al. (2011). TFEB links autophagy to lysosomal biogenesis. *Science* **332**, 1429-1433. doi:10.1126/science.1204592

Settembre, C., Zoncu, R., Medina, D. L., Vetrini, F., Erdin, S., Erdin, S., Huynh, T., Ferron, M., Karsenty, G., Vellard, M. C. et al. (2012). A lysosome-to-nucleus signalling mechanism senses and regulates the lysosome via mTOR and TFEB. *EMBO J.* **31**, 1095-1108. doi:10.1038/emboj.2012.32

Shirane, M. and Nakayama, K. I. (2006). Protrudin induces neurite formation by directional membrane trafficking. *Science* **314**, 818-821. doi:10.1126/science.1134027

Stenmark, H. (2009). Rab GTPases as coordinators of vesicle traffic. *Nat. Rev. Mol. Cell Biol.* **10**, 513-525. doi:10.1038/nrm2728

Tamura, K., Ohbayashi, N., Maruta, Y., Kanno, E., Itoh, T. and Fukuda, M. (2009). Varp is a novel Rab32/38-binding protein that regulates Tyrp1 trafficking in melanocytes. *Mol. Biol. Cell* **20**, 2900-2908. doi:10.1091/mbc.e08-12-1161

Thomas, J. D., Zhang, Y.-J., Wei, Y.-H., Cho, J.-H., Morris, L. E., Wang, H.-Y. and Zheng, X. F. S. (2014). Rab1A is an mTORC1 activator and a colorectal oncogene. *Cancer Cell* **26**, 754-769. doi:10.1016/j.ccell.2014.09.008

Wang, C., Liu, Z. and Huang, X. (2012). Rab32 is important for autophagy and lipid storage in Drosophila. *PLoS ONE* **7**, e32086. doi:10.1371/journal.pone.0032086

Wasmeier, C., Romao, M., Plowright, L., Bennett, D. C., Raposo, G. and Seabra, M. C. (2006). Rab38 and Rab32 control post-Golgi trafficking of melanogenic enzymes. *J. Cell Biol.* **175**, 271-281. doi:10.1083/jcb.200606050

Winslow, A. R., Chen, C.-W., Corrochano, S., Acevedo-Arozena, A., Gordon, D. E., Peden, A. A., Lichtenberg, M., Menzies, F. M., Ravikumar, B., Imarisio, S. et al. (2010). alpha-Synuclein impairs macroautophagy: implications for Parkinson's disease. *J. Cell Biol.* **190**, 1023-1037. doi:10.1083/jcb.201003122

Zhen, Y. and Stenmark, H. (2015). Cellular functions of Rab GTPases at a glance. *J. Cell Sci.* **128**, 3171-3176. doi:10.1242/jcs.166074